Development 140, 3435-3444 (2013) doi:10.1242/dev.089722
© 2013. Published by The Company of Biologists Ltd

The novel Rac effector RIN-1 regulates neuronal cell migration and axon pathfinding in *C. elegans*

Motomichi Doi[1,*], Hideki Minematsu[2], Yukihiko Kubota[3,‡], Kiyoji Nishiwaki[3] and Masaaki Miyamoto[2,4,*]

SUMMARY

Cell migration and axon guidance require proper regulation of the actin cytoskeleton in response to extracellular guidance cues. Rho/Rac small GTPases are essential regulators of actin remodeling. *Caenorhabditis elegans* CED-10 is a Rac1 homolog that is required for various cellular morphological changes and migration events and is under the control of several guidance signaling pathways. There is still considerable uncertainty regarding events following the activation of guidance receptors by extracellular signals and the regulation of actin dynamics based on spatiotemporally restricted Rac activity. Here we show that the VPS9 domain protein RIN-1 acts as a novel effector for CED-10 in *C. elegans*. The orthologous mammalian Rin1 protein has previously been identified as an effector for Ras GTPase and is now known to function as a guanine nucleotide exchange factor for Rab5 GTPase. We found that RIN-1 specifically binds to the GTP-bound form of CED-10 and that mutations in *rin-1* cause significant defects in migration and axon guidance of restricted neuronal cell types including AVM and HSN neurons, in contrast to the various defects observed in *ced-10* mutants. Our analyses place RIN-1 in the Slit-Robo genetic pathway that regulates repulsive signaling for dorsoventral axon guidance. In *rin-1* mutants, actin accumulated on both the ventral and dorsal sides of the developing HSN neuron, in contrast to its ventral accumulation in wild type. These results strongly suggest that RIN-1 acts as an effector for CED-10/Rac1 and regulates actin remodeling in response to restricted guidance cues.

KEY WORDS: Small GTPase, Actin remodeling, Axon pathfinding

INTRODUCTION

The spatiotemporal regulation of the activity and localization of small GTPases is determined by whether they are bound to GDP or GTP, and through interaction with effector proteins that specifically bind to the active form of the GTPase. GDP/GTP exchange factors (GEFs) that have a vacuolar protein sorting 9 (VPS9) domain mediate activation of Rab5 small GTPases by exchanging the guanine nucleotides from GDP to GTP (Carney et al., 2006). The GTP-bound active Rab5 promotes endocytic events in cells. Several VPS9 domain-containing proteins have been identified, including Rabex5 (also known as Rabgef1) (Horiuchi et al., 1997), RME-6 (Sato et al., 2005) and the Rin protein family (Tall et al., 2001; Saito et al., 2002; Kajiho et al., 2003). All of these proteins are known to directly interact with the GDP-bound form of Rab5 and to function as GEFs for Rab5. All of these VPS9 domain proteins are represented in *C. elegans*: RABX-5 (Poteryaev et al., 2010; Sann et al., 2012), RME-6 (Sato et al., 2005) and RIN-1 (this study).

The Rin protein family (Rin1, Rin2 and Rin3) has the unique property among VPS9 domain proteins of being a Ras effector that specifically binds to activated Ras (Han et al., 1997). Rin1 also exhibits Rab5-specific GEF activity, which regulates Rab5-dependent endosome fusion, EGF receptor-mediated endocytosis, insulin receptor-mediated endocytosis and IL3 receptor-dependent kinase pathways (Tall et al., 2001; Hunker et al., 2006a; Hunker et al., 2006b). In addition, Rin1 affects axon guidance of neuronal cells through physical interaction with the ephrin receptor EphA4, which acts as a repulsive guidance signal during neuronal circuit formation (Deininger et al., 2008). As a result, *Rin1*$^{-/-}$ mice show an elevated amygdala-dependent aversive memory, suggesting that Rin1 is required for inhibition of synaptic plasticity (Dhaka et al., 2003). Thus, Rin1 has important roles in the development of the nervous system; these roles are likely to be based on its function in intracellular protein transport. In addition to the protein transport function, Rin proteins are also involved in regulation of the actin cytoskeleton by directly binding to ABL tyrosine kinase. ABL proteins contain actin-binding sites and regulate cytoskeleton remodeling (Woodring et al., 2003; Hernández et al., 2004); the Rin1-ABL interaction controls the migration of epithelial cells in response to extracellular cues (Hu et al., 2005). Furthermore, the *Drosophila* Rin1 homolog Sprint regulates the localized signaling of receptor tyrosine kinases that direct border cell migration in oogenesis (Szabó et al., 2001; Jékely et al., 2005). These observations indicate that Rin proteins may mediate guidance signals that determine the actin dynamics of migrating cells or elongating axons.

This study was initiated to elucidate the precise regulatory function of Rin1 in *C. elegans* nervous system development. Rin1 homologs are conserved from nematodes to humans, suggesting indispensable roles in metazoans. We show that *C. elegans* RIN-1 specifically binds to the GTP form of CED-10, a homolog of mammalian Rac1. In *C. elegans*, *ced-10* and *mig-2*, which encodes a Rho-like GTPase, redundantly function for neuronal, vulval and gonadal cell migration (Zipkin et al., 1997; Lundquist et al., 2001; Kishore and Sundaram, 2002; Wu et al., 2002; Lundquist, 2003). Two p21-activated kinases, encoded by *pak-1* and *max-2*, that act as effectors of Rac GTPase have been shown to function redundantly with CED-10 and MIG-2 in commissural motor axon guidance

[1]Biomedical Research Institute, AIST, Tsukuba, Ibaraki 305-8566, Japan. [2]Department of Biology, Graduate School of Science, Kobe University, Kobe, Hyogo 657-8501, Japan. [3]Department of Bioscience, Kwansei Gakuin University, Sanda, Hyogo 669-1337, Japan. [4]Center for Supports to Research and Education Activities, Kobe University, Kobe, Hyogo 657-8501, Japan.

‡Present address: Department of Developmental Biology and Neurosciences, Graduate School of Life Sciences, Tohoku University, Sendai, Miyagi 980-8577, Japan
*Authors for correspondence (doi-m@aist.go.jp; miya@kobe-u.ac.jp)

Accepted 14 June 2013

(Lucanic et al., 2006). Interestingly, mutations in *ced-10*, but not *mig-2*, affect the engulfment of dead cells and cause the accumulation of cell corpses (Reddien and Horvitz, 2004; Kinchen et al., 2005; Kinchen et al., 2008). We found that *rin-1* mutants have significant defects in the axon guidance of several neuronal cell types and in muscle cell migration, and that *rin-1* acts in the same genetic pathway as *ced-10* but has a redundant function with *mig-2*. This indicates an effector function of RIN-1 for CED-10. However, *rin-1* mutants showed a less severe phenotype than *ced-10* mutants, suggesting that the effector function might be specific to restricted extracellular ligands.

MATERIALS AND METHODS

Strains

Nematodes were cultured at 20°C on standard NGM agar plates seeded with the OP50 bacterial strain as a food source. The wild-type strain Bristol N2 and several mutant strains were obtained from the Caenorhabditis Genetics Center (CGC). The *rin-1(gk431)* allele was isolated by the *C. elegans* Gene Knockout Consortium and was obtained from the CGC. The *rin-1(tk119)* allele was isolated using a PCR-based deletion screen of our original TMP-UV mutagenized library. Each newly isolated mutant allele was backcrossed more than five times to N2 wild-type animals. *ced-10(n1993)* and *ced-10(n3246)* have single amino acid changes and are weak loss-of-function mutants (Reddien and Horvitz, 2000). Homozygotes for the deletion allele *ced-10(tm597)* are sterile and are presumed null mutants. *mig-2(mu28)* is a null allele containing an early stop codon (Zipkin et al., 1997). The DD/VD neuron-labeling strain *juIs73* (an integrated line of *Punc-25::GFP*) was a kind gift from E. Lundquist (Lundquist et al., 2001). The HSN neuron-labeling strains *kyIs262* (*Punc-86::myristoylated GFP*), *kyEx1212* (*Punc-86::UNC-40::GFP*), *kyEx926* (*Punc-86::MIG-10::YFP*) and *kyEx682* (*Punc-86::GFP::actin*) were kindly provided by C. Bargmann (Adler et al., 2006). Standard genetic crosses were used to generate double- or triple-mutant animals. Each homozygous mutation was confirmed by deletion PCR or direct sequencing.

Yeast two-hybrid screening

Yeast two-hybrid screening was performed using the GAL4/AD/BD system according to the manufacturer's protocol (Clontech). A constitutively active CED-10 mutant (G12V) with a substitution in the membrane anchor region (S188C) was used as the bait, and 191,000 clones were screened. Clones that bound to the G12V form but not to the dominant-negative CED-10 mutant T17D form were selected. Interaction assays between two proteins were performed using the Matchmaker LexA system (Clontech). Each RIN-1 fragment was inserted into a pLexA bait vector and GTPases were inserted into a pB42AD prey vector. Interaction was examined by checking the growth of transformed yeast on plates lacking tryptophan, histidine, uracil and leucine, but containing 2% galactose and 1% raffinose. The mutant RIN-1 C-terminal fragments were generated as follows: the cDNA sequence corresponding to the 1350-1621 amino acid fragment was amplified by PCR and inserted into the bait vector to generate the ΔVPS from. For the ΔLeu-rich mutant, two cDNA sequences that correspond to the 1350-1543 and 1618-1889 amino acid fragments, respectively, were amplified and subcloned into the bait vector in frame. Stable expression of mutant RIN-1 proteins was confirmed by inserting GFP at the C-terminus of each mutant fragment, and fusion proteins were detected with anti-GFP antibodies (Takara). GFP fusion did not affect the interaction properties (supplementary material Fig. S1).

In vitro protein binding assays

FLAG-tagged *rin-1* cDNA was expressed in Cos-7 cells using a DEAE-dextran transfection method. Cell lysates were prepared using a lysis buffer [50 mM Tris (pH 7.5), 0.05% NP-40, 150 mM NaCl, 1 mM PMSF, 5 mM $MgCl_2$, 5 mM EDTA, 2 μg/ml leupeptin and 2 μg/ml aprotinin]. GST-fused CED-10 and Rho family GTPases were induced in 5 ml *E. coli* culture with IPTG; cells were then collected and lysed with sonication in the *E. coli* lysis buffer. The proteins were purified using glutathione Sepharose 4B (GE Healthcare Life Sciences). After nucleotide depletion at 25°C for 15 minutes in 20 mM Tris (pH 7.5), 50 mM NaCl, 2 mM EDTA and 1 mM DTT, GDP or GTP was loaded onto CED-10 and Rho family GTPases. The glutathione Sepharose suspension was combined with the Cos-7 cell lysate containing the FLAG-tagged RIN-1 protein and incubated at 4°C for 2 hours. The suspensions were precipitated, washed and boiled with SDS-containing sample buffer. Bound RIN-1 was detected by western blot analysis using anti-FLAG antibody.

Observation of cell migration and axon guidance

Neuronal cell positions, axon outgrowth and axon guidance were observed at the L4 larval stage. To visualize migration and axon guidance of the AVM neuron, the *zdIs5* strain, which harbors an integrated array of *Pmec-4::GFP*, was crossed with *rin-1* or axon guidance mutants. To analyze DD/VD neuronal morphology, each mutant was crossed with the *juIs73* strain. HSN neuronal morphology was examined by introducing the *kyIs262* transgene into each line. Localization of fluorescently labeled intracellular proteins in the developing HSN neurons was analyzed at the L2 to L3 stages, as defined by body size and stage of germline elongation. GFP fluorescent images were captured using a Zeiss LSM5 Pascal confocal laser system equipped with a 63× objective lens. All images were collected at the same laser power and detector settings using Pascal software version 3.2; they were then converted into TIFFs and manually processed using Adobe Photoshop software. Distal tip cell migration in young adults was analyzed using Nomarski microscopy. Persistent cell corpses were counted in the head region of L1 larvae at the four-cell gonad stage (Schwartz, 2007).

Molecular biology

Full-length *rin-1* cDNA was generated by ligating several partial cDNA fragments derived from yk clones (gifts from Y. Kohara, NIG, Japan); missing sequences in uncovered regions were obtained using RT-PCR. The resulting full-length cDNA was fully sequenced, and its exon and intron organization checked. For expression analysis of the *rin-1* gene, a 2.0 kb promoter region including the first exon was amplified by PCR and inserted into the pPD95.77 vector (a gift from A. Fire, Stanford School of Medicine, CA, USA). For the rescue experiments, the full-length cDNA fragment was subcloned between the *Sma*I and *Spe*I sites of pPD95.77 and a *GFP* fragment was inserted into the *Sma*I site, generating an N-terminal fusion GFP::RIN-1. Several tissue-specific promoters were inserted upstream of the GFP sequence: *myo-3* for body wall muscles, *mec-4* for mechanosensory neurons, and *unc-86* for HSN neurons. For the analysis of protein localization in the HSN neuron, the same *unc-86* promoter sequence was used for each fusion protein. All the full-length cDNAs for CED-10, RAB-5 and SAX-3 were amplified by RT-PCR and were subcloned into the pPD vectors. *GFP* or *mCherry* sequence was amplified using primers incorporating restriction enzyme sites and subcloned in frame to generate GFP::CED-10, mCherry::RAB-5 and SAX-3::GFP. All plasmids were sequenced.

Transgenic animals

Most transgenic animals were generated using standard microinjection methods. The pbLH98 [*lin-15(+)*] or *Podr-1*::RFP plasmid was used as a co-injection marker at 50 ng/μl. Each fusion plasmid was injected at 10-25 ng/μl. For the fosmid rescue experiments, the *unc-119(+)* and *Podr-1*::RFP plasmids were used as a co-injection marker. The WRM0626bB06 fosmid clone was injected at 5 ng/μl. At least three independent stable transgenic lines were used in experiments.

RESULTS

CED-10 physically interacts with the VPS9 domain protein RIN-1

To isolate potential effectors that physically bind to the GTP-bound form of CED-10, we performed a yeast two-hybrid screen using a constitutively active GTP-bound form, CED-10(G12V), as the bait. Several positive clones were identified; initially, we focused on a clone carrying part of the *C. elegans* Rin protein homolog. The physical interaction between CED-10 and RIN-1 was confirmed in *in vitro* pulldown assays and yeast two-hybrid assays. An *in vitro* pulldown assay showed that the RIN-1 protein specifically bound to CED-10 in a GTP-dependent and not in a GDP-dependent manner

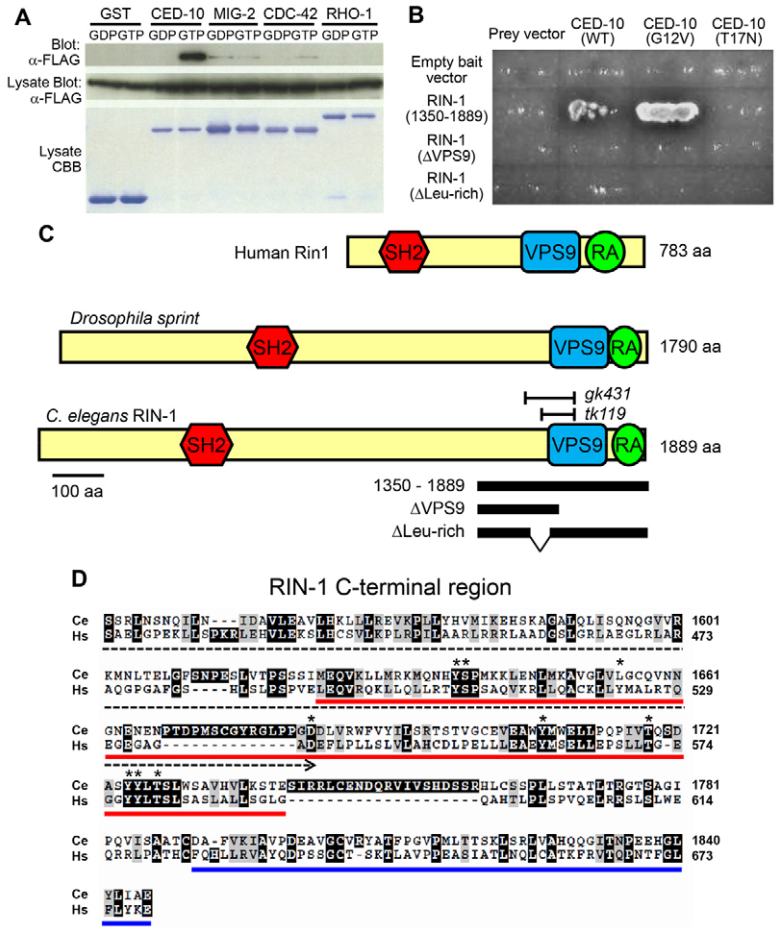

Fig. 1. *C. elegans* RIN-1 specifically interacts with the GTP-bound form of CED-10. (**A**) Pulldown binding assay using GST or the GST-fused Rho GTPase proteins. Cloned *rin-1* cDNA was expressed in Cos-7 cells and cell lysates were combined with bacterially expressed GTPases loaded with GDP or GTP. Bound RIN-1 was detected with anti-FLAG antibody. CBB, Coomassie Brilliant Blue staining. (**B**) Yeast two-hybrid analysis using the RIN-1 C-terminal fragments and CED-10. RIN-1 interacted with the constitutively active CED-10(G12V), but both the VPS9/RA region and Leu-rich region are required for the interaction with CED-10. (**C**) Protein structures of human RIN1, *Drosophila* Sprint and *C. elegans* RIN-1. SH2, Src homology domain 2; VPS9, vacuolar protein sorting homology domain 9; RA, Ras association domain. Deleted regions in the *rin-1* mutant alleles are shown above the RIN-1 structure, and protein regions used in the yeast two-hybrid assays are shown beneath; the indicated regions were introduced into the bait vector. (**D**) Amino acid alignments of the C-terminal region of *C. elegans* RIN-1 (Ce) and human RIN1 (Hs) protein. Black indicates identical amino acids; gray, similar amino acids. The VPS9 domains are underlined in red and the RA domains in blue. The region deleted in mutants is indicated by the black dashed arrow (the end point on the N-terminal side is not shown). Asterisks indicate the residues that are important for GEF activity. Note that a ~100 amino acid N-terminal region of the VPS9 domain is leucine rich and highly similar in sequence between the two proteins.

(Fig. 1A). In yeast two-hybrid analyses, the C-terminal fragment of RIN-1 bound weakly to wild-type CED-10 and strongly to the constitutively active form CED-10(G12V) (Ridley et al., 1992), but did not show any interaction with the GDP-bound form of CED-10(T17N) (Fig. 1B). Although a slight interaction was observed between RIN-1 and MIG-2 in both a GTP-dependent and GDP-dependent manner and between RIN-1 and CDC-42 in a GTP-dependent manner, RIN-1 did not bind strongly to other members of the *C. elegans* Rho/Rac family (Fig. 1A). These results suggest that RIN-1 might be a major effector for CED-10/Rac, rather than a universal effector for Rho/Rac family proteins.

Cloning of the *C. elegans* homolog of Rin1

The *C. elegans* RIN1 homolog corresponds to the C48G7.3 gene. We named this gene *rin-1* and cloned a full-length cDNA by fusing several partially cloned cDNA fragments (yk clones, gifts from Y. Kohara) and amplified RT-PCR fragments (GenBank accession number DQ344521.1). The full-length *rin-1* gene encodes a putative translated protein of 1889 amino acids (Fig. 1C). The RIN-1 protein has a similar domain structure to *Drosophila* Sprint (Szabó et al., 2001) and the mammalian Rin proteins (Han et al., 1997). All of these proteins contain an SRC homology 2 (SH2) domain in the N-terminal region, a VPS9-related domain and a Ras association (RA) domain at the C-terminus (Fig. 1C). The SH2 domain in the human RIN1 protein interacts with the cytoplasmic regions of several transmembrane receptor tyrosine kinases (Barbieri et al., 2003). The SH2 domain of *C. elegans* RIN-1 is similar to that of human RIN1 (supplementary material Fig. S2). The VPS9 domain has GDP/GTP exchange activity for Rab5 GTPase; the RA domain is where activated Ras can bind. RIN-1 shows significant similarity to human RIN1 in these two domains (Fig. 1D). We found that the C-terminal region containing the VPS9 domain interacts weakly with the GDP-bound form of RAB-5 but not with the GTP-bound form, suggesting the possibility that *C. elegans* RIN-1 can act as a GEF for RAB-5 (supplementary material Fig. S3). Furthermore, a leucine-rich region was found at the N-terminus of the VPS9 domain. The human RIN1 protein also contains this leucine-rich region at the same position and shows similarity in sequence to that of RIN-1 (Fig. 1D). Deletion of this leucine-rich region or the VPS9/RA domain prevented binding activity with CED-10 (Fig. 1B), suggesting that both the leucine-rich region and the VPS9 domain are required for the interaction between CED-10 and RIN-1. Regarding Ras, *C. elegans* RIN-1 did not bind to the *C. elegans* Ras LET-60 (data not shown).

We isolated a *rin-1* deletion allele, *tk119*, and another allele, *gk431*, has been identified by the *C. elegans* Gene Knockout Consortium (Fig. 1C). Both mutants lack the VPS9 domain and have premature stop codons in the RA domain, suggesting that the mutant proteins will lose the ability to interact with CED-10 and with RAB-5. Both alleles are likely to be strong loss-of-function mutations (see below). However, homozygous mutant animals are fertile and show no gross morphological or behavioral abnormalities. This lack of phenotypic effect is in stark contrast to the embryonic lethal phenotype of *rab-5* knockdown animals (Sato et al., 2005). Receptor-mediated endocytosis of a yolk protein in oocytes did not seem to be affected in *rin-1* mutant animals

(supplementary material Fig. S3). To date, it is not clear whether these mutations affect the regulation of RAB-5 activity, or whether *C. elegans* RIN-1 itself regulates RAB-5 activity.

Mutations in *rin-1* cause axon guidance defects in some types of neuron

To investigate the *in vivo* effects of interaction between CED-10 and RIN-1, we compared the phenotypes of *rin-1* mutants with those of *ced-10* mutants. *ced-10* mutant animals showed various defects related to cytoskeletal regulation, such as abnormalities in cell migration, axon pathfinding of neurons and phagocytosis. First, we analyzed axon outgrowth of the AVM neuron in *rin-1* mutants (Fig. 2A-E). In wild-type animals, the AVM neuron extends an axon ventrally from the cell body to the ventral nerve cord, and then elongates anteriorly to the head region (Fig. 2A). No errors in axon guidance were observed in wild-type animals. By contrast, a few *rin-*

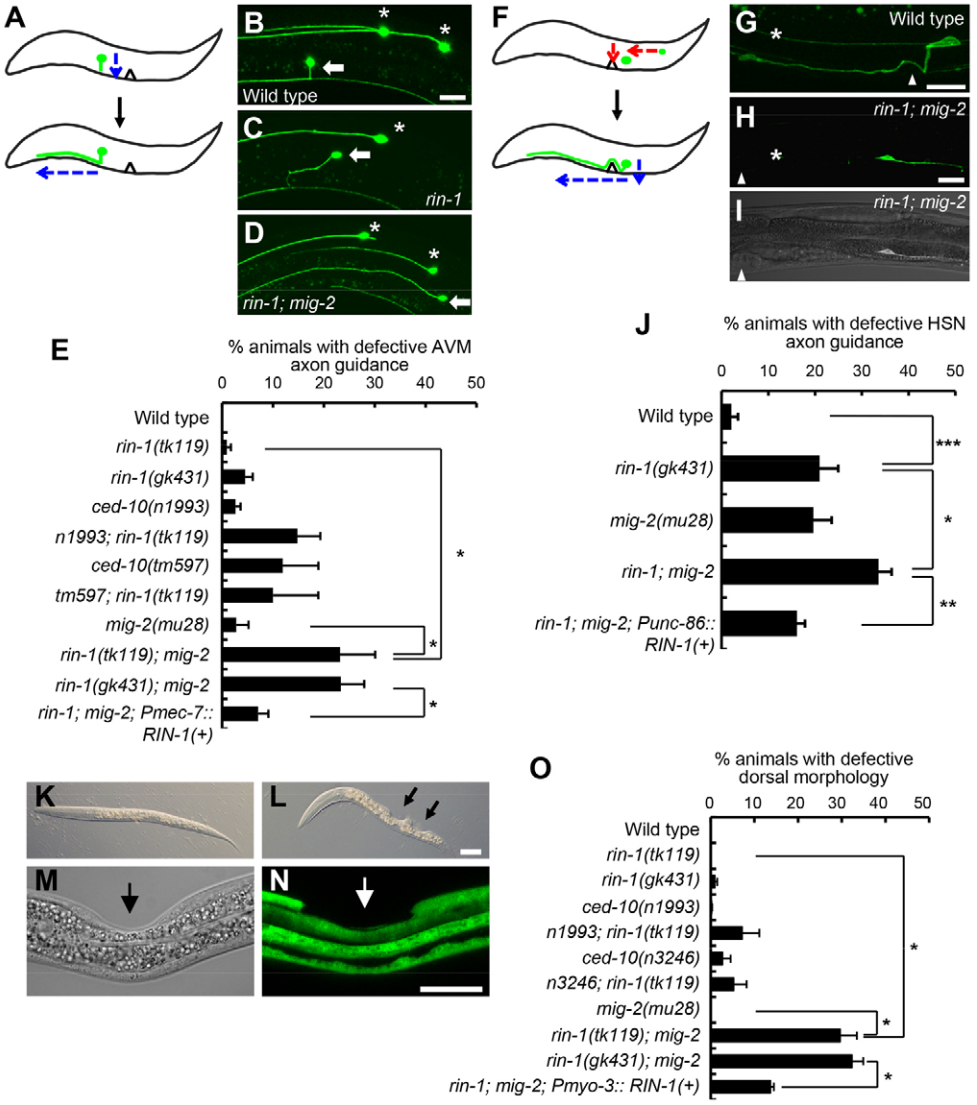

Fig. 2. *rin-1* mutations affect AVM and HSN neuron axon guidance and the migration of muscle cells. (**A-E**) Axon guidance defects in the AVM neuron. (A) Model of AVM axon guidance. Blue arrows indicate the direction of axon guidance. (B-D) Morphology of the AVM neuron in the wild type (B), *rin-1(gk431)* mutant (C) and *rin-1; mig-2* double mutant (D). Arrow indicates the AVM neuron and asterisks indicate ALM neurons. (E) Quantitative analysis of defective AVM axon guidance in *rin-1* mutants and double mutants with *ced-10* or *mig-2*. The *rin-1; mig-2* double mutants showed a significant increase in defective axon guidance compared with wild type and each single mutant. (**F-J**) Axon guidance defects in HSN neurons. (F) Model of HSN neuron development. Red arrows indicate the direction of cell migration, blue arrows the direction of axon guidance. (G) GFP image of wild type; (H) GFP image of a *rin-1; mig-2* double mutant; (I) merge of GFP and differential interference contrast (DIC) for the double mutant. Arrowhead indicates the position of the vulva and asterisk indicates the neurite of the PLM neuron. Several of the HSN neurons do not migrate close to the vulva but ceased to migrate in the posterior part of body. (J) Quantitative analysis of defective HSN axon guidance. (**K-O**) Defective dorsal morphology in *rin-1; mig-2* double mutants. (K,L) DIC images of wild-type (K) and *rin-1; mig-2* double-mutant (L) L1 larvae. Arrows indicate the position of the collapsed dorsal surface. (M,N) Muscle cells are absent in the collapsed regions of *rin-1; mig-2* double mutants. (M) DIC image of a *rin-1; mig-2* mutant carrying a *Pmyo-3::GFP* transgene; (N) reconstituted *z*-stack GFP image of the animal shown in M. A few left-dorsal body wall muscle cells are absent but right-dorsal cells appear to be located normally. (O) Quantitative analysis of the defective dorsal morphology in *rin-1* mutants, Rho/Rac mutants and double mutants. ***P<0.001, **P<0.01, *P<0.05, *t*-test; n=5 replicate experiments (in total, 95-255 animals were observed); error bars indicate s.e.m. In all images, anterior is left and ventral is bottom. Scale bars: 10 μm.

1 mutants elongated their axons in the anterior or posterior direction, rather than ventrally (Fig. 2C). Since the penetrance of single *rin-1* mutations was low, we generated double mutants with *ced-10* or *mig-2*. Double-mutant animals carrying a weak loss-of-function *ced-10(n1993)* mutation and the *rin-1* mutation showed a higher penetrance of axon guidance defects than each of the single mutants. Double mutants carrying a null *ced-10(tm597)* deletion allele and the *rin-1* mutation, however, showed a similar penetrance of axon guidance defects to the single *ced-10(tm597)* null mutant animals (Fig. 2E). These findings indicate that *rin-1* acts with *ced-10* in the same genetic pathway. We found that the axon guidance defects were significantly more common in *rin-1; mig-2* double mutants than in each single mutant. The defects in axon pathfinding were highly variable; for example, in some cases there was no ventral guidance, in others posterior elongation followed by anterior elongation, or duplicated axons (Fig. 2D; supplementary material Fig. S4). *ced-10* and *mig-2* act redundantly in neuronal cell migration and axon guidance (Lundquist et al., 2001; Kishore and Sundaram, 2002; Wu et al., 2002). We were unable to examine the phenotype of *ced-10; mig-2* double mutants owing to the very severe developmental defects shown by this genotype. However, our data suggest that *rin-1* acts in the same pathway as *ced-10* and functions redundantly with *mig-2* with regard to axon guidance of the AVM neuron. This genetic interaction is in agreement with the evidence that RIN-1 predominantly interacts with CED-10 and only slightly with MIG-2.

Similar defects in axon guidance and/or cell migration were observed in HSN neurons (Fig. 2F-J). The cell body of HSN neurons migrates anteriorly from the posterior part of the body; when it approaches the vulva, it migrates ventrally around the ventral sub-laterals where the PLN neurites are located (Fig. 2F,G). After migration, the HSN axon migrates towards the ventral nerve cord and then makes a short dorsal turn to form en passant synapses with vulval muscles and with other vulval motoneurons such as VC4 and VC5. *rin-1* mutants showed mild defects in cell body migration or axon guidance of this neuron. Some cells were located somewhat more posteriorly or dorsally compared with the wild type, and a small proportion of animals showed misrouted axon guidance, such as no ventral orientation or posterior elongation (Fig. 2H,I). *rin-1; mig-2* double mutants showed increased penetrance, indicating genetic redundancy between RIN-1 and MIG-2 signaling (Fig. 2J). These defects are unlikely to be due to slow maturation or altered developmental timing in the *rin-1* larval stages because the stage-specific developmental event of the HSN cell, such as the timing of axon elongation was unaffected in the *rin-1* mutant animals (data not shown).

rin-1 and *mig-2* redundantly affect dorsal morphology

Although gross morphological defects were not observed in *rin-1* single mutants, double mutants between *rin-1* and *ced-10* or *mig-2* exhibited abnormal dorsal morphology (Fig. 2K-O). About 25% of the *mig-2; rin-1* double mutants had one or two 'collapsed' regions at the dorsal surface, indicating that some cells had been lost from these regions (Fig. 2L). Body wall muscle-specific expression of GFP confirmed that several cells were missing from the collapsed regions in the double mutants (Fig. 2M,N). Occasionally, dorsal protrusions were also observed, but no ventral defects were seen in any of the single or double mutants (supplementary material Fig. S4). Similar to the results of the genetic analyses of axon guidance, *rin-1; ced-10(n1993)* double mutants showed increased penetrance compared with each single mutant. These results suggest that RIN-1 and CED-10 act in the same signaling pathway and that RIN-1/CED-10 signaling functions redundantly with MIG-2 signaling to maintain dorsal morphology, possibly through regulating the dorsal migration of myoblast cells.

To understand the nature of the *rin-1* mutant alleles and the results of the genetic analyses, we performed RNAi feeding knockdown experiments and compared the defects with those of the deletion mutant alleles. *rin-1(RNAi)* animals were healthy and appeared superficially wild type, as did the single *rin-1(gk431)* or *rin-1(tk119)* mutants. We also treated the *mig-2* animals with *rin-1* RNAi, and found that *rin-1(RNAi); mig-2* animals showed a similar penetrance to the *rin-1; mig-2* double mutants in both the dorsal morphology and AVM axon guidance defects (supplementary material Fig. S5). We also generated *rin-1(gk431)*/deficiency transheterozygous animals. The deficiency *yDf8*, which lacks the whole *rin-1* genomic region, was used, and *rin-1(gk431)/yDf8* animals showed similar phenotypes to the *rin-1(gk431)* allele. These data strongly suggest that the *gk431* allele is a strong loss-of-function *rin-1* mutation. Based on the phenotypic characteristics, it is likely that *tk119* is also a strong loss-of-function *rin-1* mutation.

RIN-1 functions in only some CED-10 signaling pathways

The physical interaction between RIN-1 and CED-10, and the observation that *rin-1* and *ced-10* act in the same genetic pathway, indicate that RIN-1 probably acts as a novel effector of CED-10. However, we found that several defective phenotypes observed in *ced-10* mutants were not seen in *rin-1* mutants (Table 1). *ced-10* and *mig-2* appear to act redundantly in the cell migration and axon guidance of DD/VD motoneurons, as only *ced-10; mig-2* double

Table 1. Genetic analysis of Rho/Rac signaling

Genotype	No. of persistent cell corpses	*N*	Defective DTC migration (%)	*N*	Defective DD/VD cell migration (%)	*N*
Wild type	0.2	26	0	62	0	43
rin-1(tk119)	0.2	25	3.2	63	0	47
rin-1(gk431)	0.3	16	1.5	67	0	42
ced-10(n1993)	8.4	40	28.8	59	2.0	50
ced-10(n1993); rin-1(tk119)	6.1	37	20.7	58	2.4	41
ced-10(n3246)	15.2	30	30.4	69	4.2	48
ced-10(n3246); rin-1(tk119)	14.3	25	32.3	62	4.5	44
mig-2(mu28)	0	18	49.1	55	2.2	45
rin-1(tk119); mig-2(mu28)	0	22	39	75	2.3	43
mig-2(mu28); ced-10(n1993)	ND	–	ND	–	96	25

The increased number of persistent cell corpses, defects in distal tip cell (DTC) migration and defects in DD/VD neuronal cell migration, all of which occur in the *ced-10* and/or *mig-2* mutants, were examined in *rin-1* mutants and double-mutant animals.
N, number of animals observed for each genotype; ND, not determined.

mutants show severe defects (Wu et al., 2002). However, no defects were observed in *rin-1* mutants, and no genetic interactions were found in any *rin-1* double mutants (Table 1). In *ced-10* mutant animals, many cell corpses were present at the L1 larval stage due to altered phagocytosis. However, no cell corpses were found in any of the *rin-1* mutants, suggesting that *rin-1* has no, or only a very weak, role in CED-10 signaling in phagocytosis. Furthermore, the significant defects in gonadal distal tip cell (DTC) migration observed in both *ced-10* and *mig-2* single mutants (Lundquist et al., 2001; Wu et al., 2002) were not observed in *rin-1* mutants (Table 1). These unexpected results suggest that *rin-1* might not contribute to all aspects of CED-10-mediated regulation, including apoptotic cell phagocytosis, DTC migration, DD/VD neuronal cell migration and axon pathfinding. In DTC migration, UNC-6/netrin acts as a key ligand for the UNC-40 and UNC-5 receptors, which regulate the U-shaped development of the gonad (Merz et al., 2001). Similarly, axon guidance of DD/VD motoneurons towards the dorsal side is largely dependent on UNC-6/UNC-40/UNC-5 signaling. The lack of effect on these cells in the *rin-1* mutants led us to hypothesize that RIN-1 does not act in apoptotic signaling or in UNC-6/UNC-40 guidance signaling cascades, and that RIN-1 might have a role in CED-10 activity in response to a specific extracellular signal.

RIN-1 acts in *slt-1*/*sax-3* repulsive guidance signaling

The genetic cascade regulating AVM and HSN axon guidance is well defined in *C. elegans* (Fig. 3A). Secreted ligands that provide attractive and repulsive guidance cues determine dorsoventral axon guidance of these neurons: UNC-6/netrin and its receptor UNC-40/DCC attract the axon ventrally, whereas dorsally expressed SLT-1/slit ligand and its receptor SAX-3/Robo act as a repellent signal (Wadsworth, 2002; Killeen and Sybingco, 2008). As *rin-1* seems to act in the same pathway as *ced-10* in AVM axon guidance, and *ced-10* acts in the downstream pathway of UNC-6/UNC-40 (Gitai et al., 2003), we postulated that RIN-1 might also act in this guidance signaling pathway (Fig. 3A-D).

We generated double mutants between *rin-1* and the guidance mutants, and examined axon pathfinding with respect to the AVM neuron. Interestingly, the *rin-1; unc-6* and *unc-40; rin-1* double mutants showed significantly more severe defects than the respective single mutants. Notably, more than 80% of *rin-1; unc-6* double-mutant animals showed guidance defects (Fig. 3D). By contrast, the *rin-1; slt-1* and *rin-1; sax-3* double mutants showed no significant difference to the single mutants. These data provide strong evidence that *rin-1* acts in the same genetic pathway as *slt-1/sax-3*, but acts redundantly or synergistically in the *unc-6/unc-40* pathway.

We also found that *rin-1* and *unc-40* function in different pathways for PVM cell migration. The PVM neuron is derived from the QL neuroblast and is normally located in the posterior part of the body (Fig. 3E); however, in *unc-40* mutant animals it is mislocalized to the anterior part of the body (Honigberg and Kenyon, 2000). UNC-6 does not function as the ligand for this anteroposterior axis cell migration (Fig. 3G). Although *rin-1* single mutants showed little effect, *unc-40; rin-1* double mutants exhibited a significant increase in the frequency of PVM neuron mislocalization. Thus, *rin-1* and *unc-40* act differently in both guidance of the AVM axon along the dorsoventral axis and in PVM cell migration along the anteroposterior axis. There was also evidence from molecular analyses that *rin-1* is not involved in UNC-40 signaling. UNC-40,

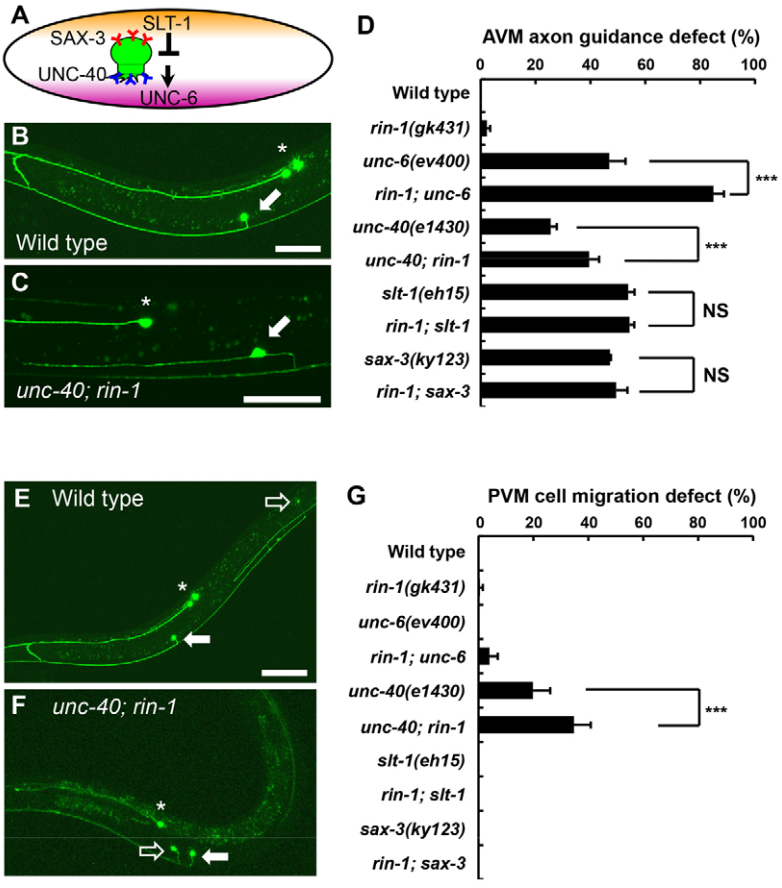

Fig. 3. *rin-1* acts in the same genetic pathway as *slt-1/sax-3* but in a distinct pathway from *unc-6/unc-40*. (**A-D**) Genetic analysis of AVM axon guidance in *rin-1* mutants and guidance mutants. (A) Illustration of the redundant axon guidance mechanisms for the AVM neuron. (B) GFP image of AVM axon guidance in a wild-type animal. (C) *rin-1; unc-40* double mutant. Closed arrows indicate the AVM neuron and asterisks indicate ALM neurons. (D) Quantitative analysis of AVM axon guidance. Both *rin-1; unc-6* and *unc-40; rin-1* double mutants show significant differences to each single mutant, suggesting that *rin-1* acts in a distinct genetic pathway from *unc-6/unc-40*. (**E-G**) The cell migration defect of the PVM neuron. (E) PVM cell position in the wild type. The PVM cell body is observed in the posterior part of the body (open arrow). (F) PVM neuron from a *rin-1; unc-40* double mutant. The cell body is located close to the AVM neuron cell body. (G) Quantitative analysis of PVM cell migration defects in *rin-1* and *unc-40* single and double mutants. The double mutants showed synergistic increases in migration defects. NS, not significant; ***$P<0.001$, *t*-test; $n=5$ replicated experiments (in total, 85-108 animals were observed); error bars indicate s.e.m. In all images, anterior is left and ventral is bottom. Scale bars: 50 μm.

DEVELOPMENT

and the downstream MIG-10 and UNC-34, predominantly localize to the ventral side of developing HSN neurons (Adler et al., 2006; Quinn et al., 2008). The asymmetric distribution of these signaling molecules probably affects CED-10 activity at elongating filopodia and regulates the site of axon formation. The localization patterns of these proteins were similar in *rin-1* mutants and wild type, indicating that RIN-1 does not affect the localization of UNC-40, UNC-34 or MIG-10 (supplementary material Fig. S7). These results suggest that RIN-1 does not function in UNC-40 signaling and, as such, presumably does not affect CED-10 activity under this guidance signaling.

RIN-1 acts cell-autonomously and is expressed in a cell type-specific and stage-specific manner

To examine whether RIN-1 function is required for AVM and HSN neurons and muscle cells themselves, we expressed the GFP::RIN-1 fusion protein under the control of cell type-specific promoters. GFP::RIN-1 partially rescued the defects in the AVM and HSN neurons and in muscles in *rin-1* mutants (Fig. 2E,J,O). These results indicate that RIN-1 has a cell-autonomous function in migrating cells and in axon-elongating neurons.

The fusion protein accumulated in a punctate pattern in the body wall muscles, AVM and PLM neuronal cell bodies of mature animals, although a diffuse distribution was also seen in the cytoplasmic region (Fig. 4A-E). However, these localization patterns do not seem to reflect protein function during cytoskeletal regulation when cells are migrating or axons are elongating. Thus, we also examined the localization pattern of the RIN-1 protein in the developing HSN neurons. The fusion protein showed punctate expression that was mostly localized towards the periphery of the cells (Fig. 4F). One or two large areas of signal were observed at the center of cells, the nature of which is unknown. A punctate distribution was also observed in elongating filopodia-like structures. There was no indication of preferential protein accumulation at the ventral or dorsal sides; rather, the fluorescent signals were uniformly distributed at the cell margin. Most GFP foci were observed in regions distinct from RAB-5-positive early or late endosomes, as labeled with mCherry::RAB-5 (Fig. 4H-J). Thus, RIN-1 protein probably accumulates on, or just beneath, the plasma membrane during these stages of development. The localization patterns of the RIN-1 protein were remained largely unaltered in the *ced-10(tm597)* null mutant background (Fig. 4G), indicating that RIN-1 localization is not dependent on CED-10.

Although we examined *rin-1* expression using a *rin-1* promoter-GFP fusion construct, GFP was not detected in the cells in which we had shown that cell-autonomous RIN-1 activity is required, suggesting that our construct failed to report the endogenous expression of *rin-1* (supplementary material Fig. S6).

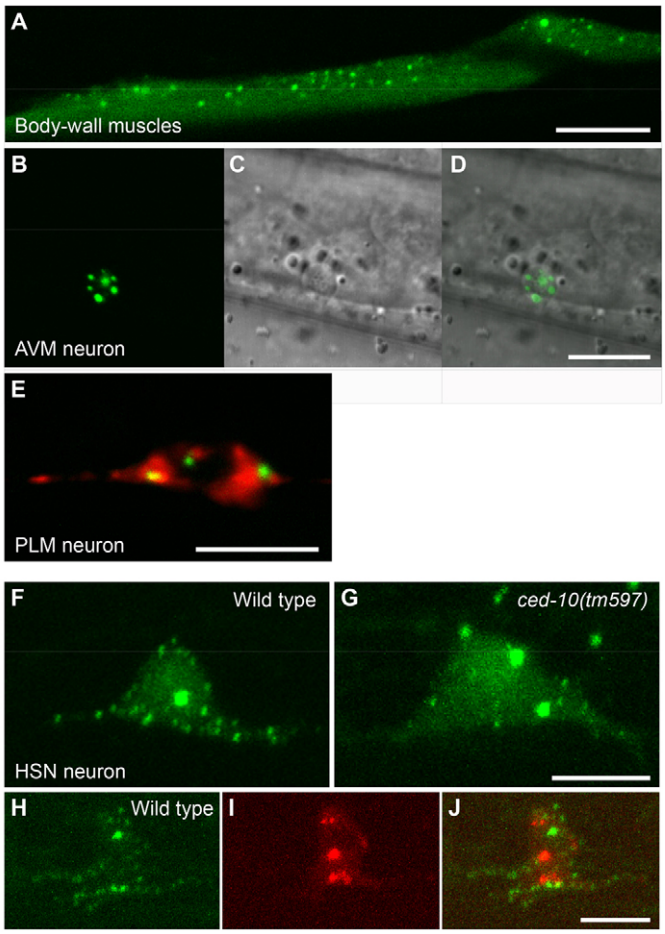

Fig. 4. RIN-1 protein localizes at the periphery of the developing HSN neuron. Localization patterns of RIN-1 protein in mature animals (A-E) and migrating cells (F-J). The GFP::RIN-1 fusion protein was expressed in the body wall muscle or neuronal cells under the control of different cell type-specific promoters. (**A**) Body wall muscles. The fusion protein was diffusely distributed in the cells, but accumulated strongly in unidentified small compartments. (**B-D**) AVM neuron. (B) GFP image; (C) DIC image; (D) merge of GFP and DIC. A few strong foci were observed in the cell body. (**E**) PLM neuron. The mCherry::RAB-5 fusion protein, which labels early or late endosomes, was simultaneously expressed. (**F**,**G**) Localization patterns of GFP::RIN-1 fusion protein in developing HSN neurons (L3 stage) of wild type (F) and *ced-10(tm597)* (G). GFP signals are seen in punctate structures near the periphery of the cell. (**H-J**) Localization patterns of GFP::RIN-1 and mCherry::RAB-5 fusion proteins. (H) GFP::RIN-1, (I) mCherry::RAB-5, (J) merge. Most GFP signals were seen near the cell margin or in filopodia-like structures where RAB-5 is not localized. In all images, anterior is left and ventral is bottom. Scale bars: 10 μm.

Actin mislocalization in migrating HSN neurons of *rin-1* mutants

The cell migration and axon guidance defects observed in *rin-1* mutants suggested that actin organization or disorganization at specific sites might be affected through the disruption of CED-10 signaling. To examine this, a GFP::actin fusion protein was expressed in HSN neurons (Adler et al., 2006). In wild-type animals, strong GFP fluorescence was normally observed in filopodia-like structures elongating in the anterior-ventral direction where the synaptic target of the HSN axon is located (Fig. 5A,B). In very few cases, a weak GFP signal was observed in dorsal retraction fibers. In *rin-1* mutants, however, the ectopic accumulation of the GFP fusion protein at dorsal or posterior filopodia (or retracting fibers) was significantly increased (Fig. 5C,D,G). The strong HSN axon guidance defects in *rin-1; mig-2* double mutants were mirrored by enrichment of GFP::actin in large lamellipodia-like structures on the posterior side of the cells, which is the opposite direction to normal HSN axon outgrowth (Fig. 5E,F). The defect was rescued by the HSN cell-specific expression of RIN-1, again suggesting a cell-autonomous function of RIN-1 (Fig. 5G). These results strongly indicate that the regulation of actin dynamics is disrupted in *rin-1* mutants, and that this may affect the migration of neuronal and myoblast cells, as well as the direction of axon guidance in several neuron types.

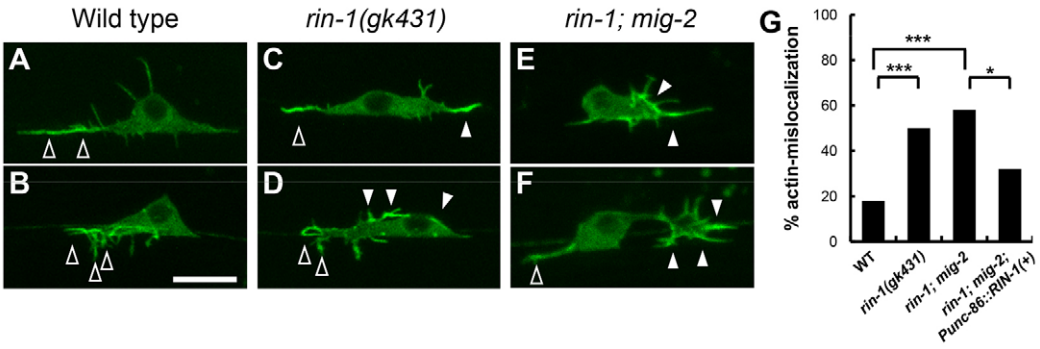

Fig. 5. RIN-1 regulates actin localization in the developing HSN neuron. (**A-F**) Localization patterns of GFP::actin fusion protein in the developing HSN neurons of wild type (A,B), *rin-1(gk431)* mutants (C,D) and *rin-1; mig-2* double mutants (E,F). Open arrowheads indicate normal actin accumulation at the anterior/ventral side of the cell body. Closed arrowheads indicate mislocalized actin at the posterior/dorsal side as observed in *rin-1* or *rin-1; mig-2* mutants. (**G**) Quantitative analysis of mislocalized actin. ***P<0.001, *P<0.05, χ^2-test; n=100 animals. Scale bars: 10 μm.

RIN-1 acts with CED-10 in the regulation of filopodia formation

To explore more clearly how RIN-1 and CED-10 cooperate in cells, we expressed a GFP::CED-10 fusion protein in developing HSN neurons and compared its localization pattern in wild type and *rin-1* mutants. During migration of an HSN cell (from L2 to L3 stages) or the elongation of its axon (L3 to early L4 stages), CED-10 is localized uniformly in the cell (Fig. 6A-D). No obvious difference in localization patterns was found at any developmental stages between *rin-1* mutant and wild-type animals. Given that RIN-1 binds specifically to the GTP-bound form of CED-10, we examined the localization pattern of the constitutively active form, CED-10(G12V). CED-10(G12V) and wild-type CED-10 displayed similar localization patterns, and no difference was observed in the *rin-1* mutants, suggesting that RIN-1 does not affect the localization of the active form of CED-10 (Fig. 6E-H).

Even though CED-10 seemed to be localized normally in *rin-1* mutants, we found that *rin-1* mutants showed a clear response to the expression of the active form of CED-10 (Fig. 6F,H). In wild-type animals, the active form of CED-10 caused ectopic neurite formation around the cell body, and some were extended from the posterior side of the cells (Fig. 6E,G). In *rin-1* mutants, the number of filopodia-like structures was significantly increased: from an average per cell of 6.5±0.5 in wild-type animals to 12.1±1.1 in *rin-1* mutants (n>20, P<0.001 by Student's t-test). These results strongly suggest that RIN-1 functions in CED-10 signaling for the regulation of filopodia formation at restricted sites of migrating or axon-elongating cells.

DISCUSSION

Our findings show that RIN-1 is a novel effector of CED-10, and that this interaction is required for directed migration and axon guidance by regulating the formation of filopodia in restricted membrane regions of several cell types. Our phenotypic and genetic analyses suggest that this effector function of RIN-1 is dependent on specific extracellular signals. In engulfing cells, such as the hypodermis, RIN-1 is not required for the CED-10 activity that regulates cellular morphological changes for phagocytosis under the 'eat-me' signal from dying cells. Similarly, the UNC-6 ligand does not seem to activate RIN-1 as an effector of CED-10 in DTC migration, although transient expression of *rin-1* was observed in both the hypodermis and DTC (supplementary material Fig. S6). In DD/VD neurons, since no defects were observed in *rin-1* mutants and no expression of *rin-1* was seen, other regulators such as PAK-1 and MAX-2 probably function for CED-10 activity (Lucanic et al., 2006). In our study, only the SLT-1 signal could be demonstrated to be a functional extracellular cue of RIN-1 for CED-10 activity in cell and axon migration.

These findings led us to propose the model of RIN-1 function in actin regulation in cell migration and axon guidance shown in Fig. 7. In this model, RIN-1 binds to the active form of CED-10 and downregulates its activity by an unknown mechanism. RIN-1

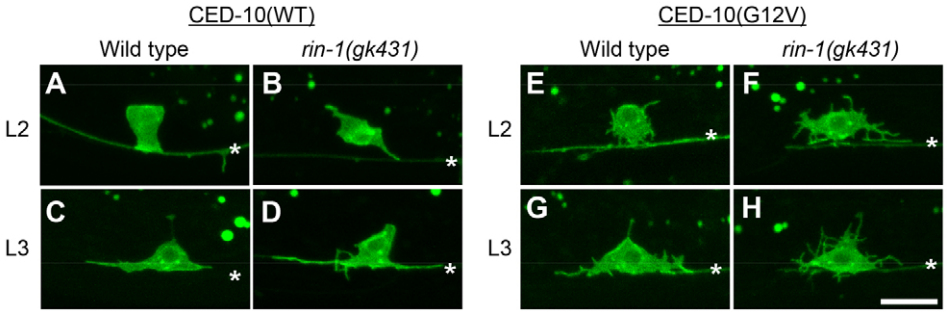

Fig. 6. RIN-1 regulates filopodia formation through interaction with the GTP-bound form of CED-10. Expression patterns of CED-10::GFP fusion protein and morphological changes in the developing HSN neuron. (**A-D**) Expression of the wild-type CED-10 fusion protein in wild type (A,C) or *rin-1(gk431)* (B,D) at the late L2 larval stage (A,B) or mid-L3 larval stage (C,D). Note the long posterior-directed filopodia in the *rin-1* mutants. (**E-H**) Expression of the constitutively active form CED-10(G12V) induces excess formation of filopodia-like structures at various regions of the cell. Asterisks indicate the neurite of the PLM neuron. Scale bar: 10 μm.

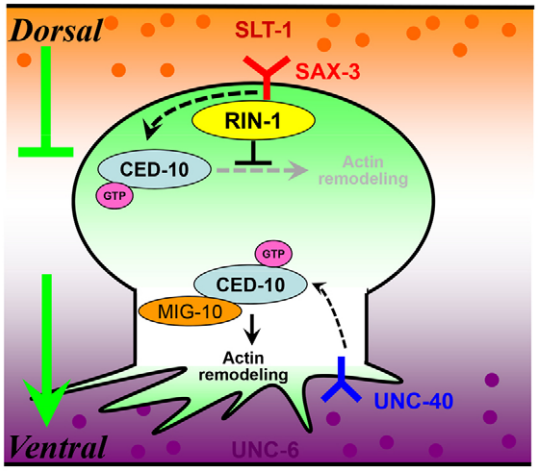

Fig. 7. Model of RIN-1 function in cell migration and/or axon guidance. RIN-1 may downregulate CED-10 activity by directly binding to the active form of the protein. In dorsoventral axis cell migration, dorsally secreted SLT-1 ligands bind to the SAX-3 receptor, and SAX-3 activation leads to the activation of CED-10 by converting it to the GTP-bound form. RIN-1, which might be regulated by SAX-3, specifically binds to and downregulates the activated CED-10 in regions where the repulsive guidance signals are highly concentrated. This downregulation might suppress excess filopodia and/or lamellipodia formation at these sites. RIN-1 does not affect the activity of CED-10 on the ventral side. The ventral CED-10 could be activated by the UNC-6 signal through the UNC-40 receptor.

protein has a punctate distribution on both the dorsal and ventral sides of developing HSN neurons. If the RIN-1 on both sides of the cell is activated, then filopodia formation on the axon-elongating side may be suppressed and the cells cannot achieve proper axon guidance. By this means, RIN-1 regulation of CED-10 activity should occur at the site where there is sufficient target ligand to activate RIN-1. In HSN neurons, the SLT-1 concentration on the dorsal side is high along the dorsoventral axis gradient and, as such, RIN-1 may only be activated on this side. In *rin-1* mutants, the truncated RIN-1 protein that lacks the VPS9/RA domain did not bind to CED-10 and this absence of interaction with CED-10 caused a failure to inhibit ectopic actin accumulation and filopodia formation on the dorsal/posterior sides of the cells. We conclude that RIN-1 is probably a negative regulator of CED-10 under SLT-1/SAX-3 repellent guidance signaling for AVM and HSN neurons. The ligands for dorsal myoblast migration and posterior migration of PVM neurons have not yet been identified; however, these signals could also affect RIN-1 interaction with CED-10.

In addition to this negative regulator model, we cannot exclude the possibility that RIN-1 regulates intracellular transport of signaling molecules required for cell migration. For example, recruitment of activated CED-10 might be slightly altered in the developing HSN neurons of *rin-1* mutants, although defects in CED-10 localization were not apparent in *rin-1* mutant animals. Alternatively, dynamic recruitment of active CED-10 might occur at a restricted site and time point when cells receive the requisite amount of ligand. Another possible RIN-1 function in cell migration and axon guidance is in the regulation of receptor endocytosis from the plasma membrane. Previous studies have shown that human RIN1 preferentially regulates internalization of tyrosine kinase-type transmembrane receptors in a ligand-dependent manner (Barbieri et al., 2003). Mouse Rin1 has been shown to physically interact with the ephrin receptor EphA4 and to affect its intracellular endocytosis, probably via Rab5 activation (Deininger et al., 2008). Since both the UNC-40 and SAX-3 guidance receptors function in axon guidance of the AVM and HSN neurons, RIN-1 might interact with, and regulate the internalization of, these receptors. In the HSN neuron of *rin-1* mutants, however, the UNC-40 or SAX-3 GFP-fusion proteins appeared to be expressed normally and showed a typical localization pattern (supplementary material Fig. S7). Further experiments are required to determine the precise roles of RIN-1 in guidance receptor-mediated cell responses, in addition to the analysis of RAB-5 GEF function.

The most interesting finding regarding Rin proteins is that RIN-1 has the potential to interact with multiple small GTPases. Regarding Ras, however, RIN-1 did not physically bind to the *C. elegans* Ras LET-60, and *rin-1* mutants did not show any obvious defects relating to Ras signaling and any genetic interaction with the *let-60(gf)* mutation (data not shown). Although it has a highly conserved RA domain, our results suggest that *C. elegans* RIN-1 is not a Ras-interacting protein. Rather, our study suggests that RIN-1 could be a component in the functional crosstalk among the small GTPases, which regulate several cellular events. Another recent study also proposed crosstalk between Rab5 and Rac1: Rab5-mediated endocytosis is required for the activation of Rac by extracellular stimuli, leading to spatially restricted actin remodeling for cell migration or lamellipodia formation (Palamidessi et al., 2008). The binding of the ligand to its receptor stimulates endocytosis of the receptor and Rac-GEF complex, and subsequent Rac activation as a result of GDP hydrolysis in the endosomes. We have shown that RIN-1 and CED-10 can interact directly through the region that includes the VPS9 domain, to which RAB-5 also binds. Therefore, RIN-1 might act as a crosstalk mediator between RAB-5 and CED-10.

In conclusion, we have described a novel mechanism through which RIN-1 regulates actin dynamics via direct interaction with Rac. This interaction might determine the site of filopodia formation on the cell surface in migrating neurons and developing axons.

Acknowledgements
We thank C. Bargmann for the HSN-labeling strains; E. Lundquist for the *juls73* strain; A. Fire for the pPD plasmids; Y. Kohara for cDNA clones; N. Matsuyama and E. Suzuki for technical assistance in molecular cloning and genetic crossing; E. Lundquist and members in the Molecular Neurobiology Group in AIST for discussion and comments on the manuscript. Some strains were provided by the Caenorhabditis Genetics Center (CGC), which is funded by the NIH Office of Research Infrastructure Programs [P40 OD010440].

Funding
This work was supported by a Japan Society for the Promotion of Science (JSPS) KAKENHI to M.D.

Competing interests statement
The authors declare no competing financial interests.

Author contributions
M.D. designed the project, performed most of the experiments and wrote the manuscript. H.M. carried the yeast two-hybrid screening. Y.K. carried out the genetic experiments and commented on the manuscript. K.N. designed the project and wrote the manuscript. M.M. designed the project, carried out the biochemical experiments and wrote the manuscript.

Supplementary material
Supplementary material available online at
http://dev.biologists.org/lookup/suppl/doi:10.1242/dev.089722/-/DC1

References
Adler, C. E., Fetter, R. D. and Bargmann, C. I. (2006). UNC-6/Netrin induces neuronal asymmetry and defines the site of axon formation. *Nat. Neurosci.* **9**, 511-518.

Barbieri, M. A., Kong, C., Chen, P. I., Horazdovsky, B. F. and Stahl, P. D. (2003). The SRC homology 2 domain of Rin1 mediates its binding to the epidermal growth factor receptor and regulates receptor endocytosis. *J. Biol. Chem.* **278**, 32027-32036.
Calixto, A., Chelur, D., Topalidou, I., Chen, X. and Chalfie, M. (2010). Enhanced neuronal RNAi in C. elegans using SID-1. *Nat. Methods* **7**, 554-559.
Carney, D. S., Davies, B. A. and Horazdovsky, B. F. (2006). Vps9 domain-containing proteins: activators of Rab5 GTPases from yeast to neurons. *Trends Cell Biol.* **16**, 27-35.
Deininger, K., Eder, M., Kramer, E. R., Zieglgänsberger, W., Dodt, H. U., Dornmair, K., Colicelli, J. and Klein, R. (2008). The Rab5 guanylate exchange factor Rin1 regulates endocytosis of the EphA4 receptor in mature excitatory neurons. *Proc. Natl. Acad. Sci. USA* **105**, 12539-12544.
Dhaka, A., Costa, R. M., Hu, H., Irvin, D. K., Patel, A., Kornblum, H. I., Silva, A. J., O'Dell, T. J. and Colicelli, J. (2003). The RAS effector RIN1 modulates the formation of aversive memories. *J. Neurosci.* **23**, 748-757.
Gitai, Z., Yu, T. W., Lundquist, E. A., Tessier-Lavigne, M. and Bargmann, C. I. (2003). The netrin receptor UNC-40/DCC stimulates axon attraction and outgrowth through enabled and, in parallel, Rac and UNC-115/AbLIM. *Neuron* **37**, 53-65.
Grant, B. and Hirsh, D. (1999). Receptor-mediated endocytosis in the Caenorhabditis elegans oocyte. *Mol. Biol. Cell* **10**, 4311-4326.
Han, L., Wong, D., Dhaka, A., Afar, D., White, M., Xie, W., Herschman, H., Witte, O. and Colicelli, J. (1997). Protein binding and signaling properties of RIN1 suggest a unique effector function. *Proc. Natl. Acad. Sci. USA* **94**, 4954-4959.
Hernández, S. E., Krishnaswami, M., Miller, A. L. and Koleske, A. J. (2004). How do Abl family kinases regulate cell shape and movement? *Trends Cell Biol.* **14**, 36-44.
Honigberg, L. and Kenyon, C. (2000). Establishment of left/right asymmetry in neuroblast migration by UNC-40/DCC, UNC-73/Trio and DPY-19 proteins in C. elegans. *Development* **127**, 4655-4668.
Horiuchi, H., Lippé, R., McBride, H. M., Rubino, M., Woodman, P., Stenmark, H., Rybin, V., Wilm, M., Ashman, K., Mann, M. et al. (1997). A novel Rab5 GDP/GTP exchange factor complexed to Rabaptin-5 links nucleotide exchange to effector recruitment and function. *Cell* **90**, 1149-1159.
Hu, H., Bliss, J. M., Wang, Y. and Colicelli, J. (2005). RIN1 is an ABL tyrosine kinase activator and a regulator of epithelial-cell adhesion and migration. *Curr. Biol.* **15**, 815-823.
Hunker, C. M., Galvis, A., Veisaga, M. L. and Barbieri, M. A. (2006a). Rin1 is a negative regulator of the IL3 receptor signal transduction pathways. *Anticancer Res.* **26** 2A, 905-916.
Hunker, C. M., Giambini, H., Galvis, A., Hall, J., Kruk, I., Veisaga, M. L. and Barbieri, M. A. (2006b). Rin1 regulates insulin receptor signal transduction pathways. *Exp. Cell Res.* **312**, 1106-1118.
Jékely, G., Sung, H. H., Luque, C. M. and Rørth, P. (2005). Regulators of endocytosis maintain localized receptor tyrosine kinase signaling in guided migration. *Dev. Cell* **9**, 197-207.
Kajiho, H., Saito, K., Tsujita, K., Kontani, K., Araki, Y., Kurosu, H. and Katada, T. (2003). RIN3: a novel Rab5 GEF interacting with amphiphysin II involved in the early endocytic pathway. *J. Cell Sci.* **116**, 4159-4168.
Killeen, M. T. and Sybingco, S. S. (2008). Netrin, Slit and Wnt receptors allow axons to choose the axis of migration. *Dev. Biol.* **323**, 143-151.
Kinchen, J. M., Cabello, J., Klingele, D., Wong, K., Feichtinger, R., Schnabel, H., Schnabel, R. and Hengartner, M. O. (2005). Two pathways converge at CED-10 to mediate actin rearrangement and corpse removal in C. elegans. *Nature* **434**, 93-99.
Kinchen, J. M., Doukoumetzidis, K., Almendinger, J., Stergiou, L., Tosello-Trampont, A., Sifri, C. D., Hengartner, M. O. and Ravichandran, K. S. (2008). A pathway for phagosome maturation during engulfment of apoptotic cells. *Nat. Cell Biol.* **10**, 556-566.
Kishore, R. S. and Sundaram, M. V. (2002). ced-10 Rac and mig-2 function redundantly and act with unc-73 trio to control the orientation of vulval cell divisions and migrations in Caenorhabditis elegans. *Dev. Biol.* **241**, 339-348.
Lucanic, M., Kiley, M., Ashcroft, N., L'etoile, N. and Cheng, H. J. (2006). The Caenorhabditis elegans P21-activated kinases are differentially required for UNC-6/netrin-mediated commissural motor axon guidance. *Development* **133**, 4549-4559.
Lundquist, E. A. (2003). Rac proteins and the control of axon development. *Curr. Opin. Neurobiol.* **13**, 384-390.
Lundquist, E. A., Reddien, P. W., Hartwieg, E., Horvitz, H. R. and Bargmann, C. I. (2001). Three C. elegans Rac proteins and several alternative Rac regulators control axon guidance, cell migration and apoptotic cell phagocytosis. *Development* **128**, 4475-4488.
Merz, D. C., Zheng, H., Killeen, M. T., Krizus, A. and Culotti, J. G. (2001). Multiple signaling mechanisms of the UNC-6/netrin receptors UNC-5 and UNC-40/DCC in vivo. *Genetics* **158**, 1071-1080.
Palamidessi, A., Frittoli, E., Garré, M., Faretta, M., Mione, M., Testa, I., Diaspro, A., Lanzetti, L., Scita, G. and Di Fiore, P. P. (2008). Endocytic trafficking of Rac is required for the spatial restriction of signaling in cell migration. *Cell* **134**, 135-147.
Poteryaev, D., Datta, S., Ackema, K., Zerial, M. and Spang, A. (2010). Identification of the switch in early-to-late endosome transition. *Cell* **141**, 497-508.
Quinn, C. C., Pfeil, D. S. and Wadsworth, W. G. (2008). CED-10/Rac1 mediates axon guidance by regulating the asymmetric distribution of MIG-10/lamellipodin. *Curr. Biol.* **18**, 808-813.
Reddien, P. W. and Horvitz, H. R. (2000). CED-2/CrkII and CED-10/Rac control phagocytosis and cell migration in Caenorhabditis elegans. *Nat. Cell Biol.* **2**, 131-136.
Reddien, P. W. and Horvitz, H. R. (2004). The engulfment process of programmed cell death in Caenorhabditis elegans. *Annu. Rev. Cell Dev. Biol.* **20**, 193-221.
Ridley, A. J., Paterson, H. F., Johnston, C. L., Diekmann, D. and Hall, A. (1992). The small GTP-binding protein rac regulates growth factor-induced membrane ruffling. *Cell* **70**, 401-410.
Saito, K., Murai, J., Kajiho, H., Kontani, K., Kurosu, H. and Katada, T. (2002). A novel binding protein composed of homophilic tetramer exhibits unique properties for the small GTPase Rab5. *J. Biol. Chem.* **277**, 3412-3418.
Sann, S. B., Crane, M. M., Lu, H. and Jin, Y. (2012). Rabx-5 regulates RAB-5 early endosomal compartments and synaptic vesicles in C. elegans. *PLoS ONE* **7**, e37930.
Sato, M., Sato, K., Fonarev, P., Huang, C. J., Liou, W. and Grant, B. D. (2005). Caenorhabditis elegans RME-6 is a novel regulator of RAB-5 at the clathrin-coated pit. *Nat. Cell Biol.* **7**, 559-569.
Schwartz, H. T. (2007). A protocol describing pharynx counts and a review of other assays of apoptotic cell death in the nematode worm Caenorhabditis elegans. *Nat. Protoc.* **2**, 705-714.
Szabó, K., Jékely, G. and Rørth, P. (2001). Cloning and expression of sprint, a Drosophila homologue of RIN1. *Mech. Dev.* **101**, 259-262.
Tall, G. G., Barbieri, M. A., Stahl, P. D. and Horazdovsky, B. F. (2001). Ras-activated endocytosis is mediated by the Rab5 guanine nucleotide exchange activity of RIN1. *Dev. Cell* **1**, 73-82.
Wadsworth, W. G. (2002). Moving around in a worm: netrin UNC-6 and circumferential axon guidance in C. elegans. *Trends Neurosci.* **25**, 423-429.
Woodring, P. J., Hunter, T. and Wang, J. Y. (2003). Regulation of F-actin-dependent processes by the Abl family of tyrosine kinases. *J. Cell Sci.* **116**, 2613-2626.
Wu, Y. C., Cheng, T. W., Lee, M. C. and Weng, N. Y. (2002). Distinct rac activation pathways control Caenorhabditis elegans cell migration and axon outgrowth. *Dev. Biol.* **250**, 145-155.
Zipkin, I. D., Kindt, R. M. and Kenyon, C. J. (1997). Role of a new Rho family member in cell migration and axon guidance in C. elegans. *Cell* **90**, 883-894.